2nd IFAC Workshop on Automatic Control in Offshore Oil and Gas Production,
May 27-29, 2015, Florianópolis, Brazil

Automated Dual Gradient Drilling and its Parametric Analysis during Connection ⋆

D. Sui * **O. G. H. Nygaard** *

* *Department of Petroleum Engineering, University of Stavanger, Stavanger, Norway(e-mail: dan.sui@uis.no).*

Abstract: Since Dual Gradient Drilling (DGD) is a new and advanced drilling technology, currently its methods, procedures, simulations and experiments are still underdeveloped. It requires more study, research and advanced methods on DGD systems. The motivation of the paper is to study DGD systems, design good operational drilling parameters, and work on automated DGD systems to further realize safe and efficient drilling. This paper aims to implement automated DGD systems by regulating the mud level in the riser to maintain the stable bottom hole pressure during connection operations. Furthermore, the sensitivity analysis of parameters is included and good configuration parameters are recommended.

1. INTRODUCTION

As oilfields are ageing and depleting, operators are forced to start searching for oil in more hostile and challenging environments. These new environments will introduce and lead to severe drilling challenges and potential problems. Prospects like ultra-deep water reservoirs and depleted offshore reservoirs are difficult to drill with conventional drilling. This has led the industry to developing advanced drilling technologies, like Managed Pressure Drilling and Dual Gradient Drilling (DGD),see for instance, Zhou and Nygaard (2011); Forrest and Bailey (2001); Breyholtz et al. (2009); Schumacher et al. (2002); Zhou et al. (2008); Stamnes et al. (2008); Nygaard et al. (2007).

DGD is an unconventional drilling method and it is classified as a Managed Pressure Drilling technique. In a DGD system, the hydrostatic gradient in the wellbore is composed of two parts. In the upper part above the seabed the light mud is often used; in the lower part below the seabed the heavy mud is chosen. By using fluids with varying densities, DGD can effectively manage the downhole pressure to obtain a pressure profile that often fits much better in between the pore and fracture gradients making it possible to drill much deeper before setting casing.

During conventional drilling, before a connection is made, the mud circulation has to be stopped. This causes a rapid drop in the bottom hole pressure due to the changes in pressure loss. Such quick pressure drop may put the wellbore at risk. For instance, some potential drilling problems, like formation fracturing, formation ballooning, lost circulation, connection kick and formation collapse, differential sticking, stuck pipe, and slugging of cuttings return may be encountered when the main pump is shut down during a connection procedure. By utilizing DGD systems the bottom hole pressure variation related to connection operations can be significantly reduced by managing the mud level in the riser or the flow rate of the subsea mud pump. Although this new technology has several advantages over conventional drilling, it has its limits and challenges. The limited use of DGD makes it difficult to adapt to this new drilling method. Moreover procedures and equipment developed have had limited proof of reliability and viability, which have created a drive for more study, research and experiences on DGD systems.

This paper aims to study automated DGD system during connection operations. Furthermore, the work focuses on the sensitivity analysis of parameters affecting DGD systems, considers several relevant models (hydraulic model, density model, etc.) and implements control strategies to realize the automated DGD technique. Similar work about sensitivity analysis of DGD systems has been studied in Sigurjonsson (2011); Time (2014); Hanekamhaug (2015); Gaup (2012).

In the sensitivity analysis, the effect of drilling parameters on DGD systems, such as flow rate of main pump, mud weight, geometry of riser is analyzed. Then suitable/good configuration parameters, for instance, the density of light liquid filled in the upper part of the riser is recommended. Model predictive control (MPC) strategy (Garcia and Prett (1989); Mayne and Michalska (1990)) is employed to maintain the stable bottom hole pressure (BHP) during connection operations by manipulating heavy mud level in the riser. MPC is an advanced optimal strategy that deals with controller design for industrial process systems. In the last decade, researchers have drawn more attraction to the MPC methodology applied in the drilling field, especially in managed pressure drilling and dual gradient drilling, see Breyholtz et al. (2011); Godhavn et al. (2013).

Results will be presented in the simulations, where the methodology illustrates a potential behavior of automated DGD systems. It will give helpful decision support and drilling efficiency and make safe drilling. In this paper, the following abbreviations are used:
DGD: dual gradient drilling
BHP: bottom hole pressure
MPC: model predictive control

2. DUAL GRADIENT DRILLING

The drilling system used in this paper is illustrated in Figure 1. The drill string and annulus are treated as two separate control volumes that are connected through the drill bit's check valve. The DGD system uses two pumps to circulate the mud. The main pump pumps the mud downward through the drill pipe, through the drill collars, through small holes in the drill bit,

⋆ This work was supported in part by Petroleum Engineering Department, University of Stavanger and the Statoil Akademia program

back up the annulus to the riser. The mud is back to the surface using a subsea pump which pumps the mud to the rig through a separated mud return line so as to be re-circulated. The mud level in the riser is somewhere between the seabed and the sea level. The light liquid is filled into the riser from the surface and is above the mud level. Sometimes fill pump or booster pump can be used in the DGD system which allows for the mud level increasing quickly when an increase in BHP is required. To illustrate the system more easily and clear, the parameters used in the DGD system are given in Table 1.

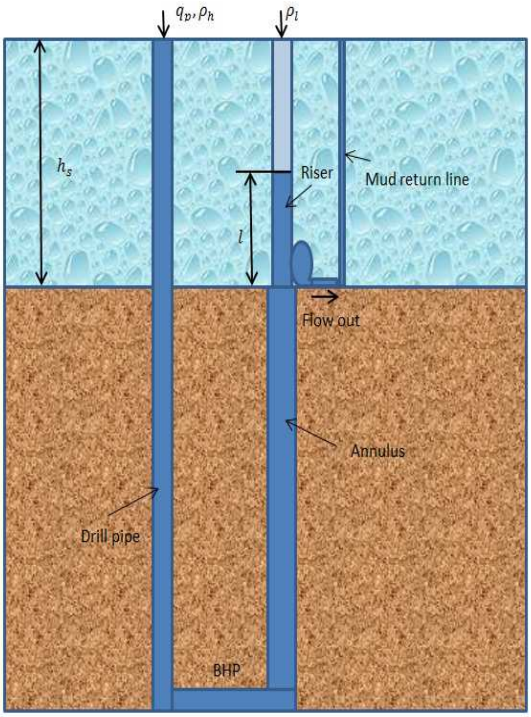

Fig. 1. A simplified drawing of the DGD drilling system.

3. MODELLING

3.1 Pressure loss model

During circulation of drilling fluids, the pressure in the wellbore consists of two components, the hydrostatic pressure and the dynamic fluid pressure loss. Frictional pressure loss is a function of several factors

- fluid rheological behavior and properties (e.g. viscosity, density, etc.)
- flow regime (laminar, transitional or turbulent flow)
- flow rate
- wellbore geometry and drillstring configuration

The pressure loss is directly proportional to its length, the fluid density, the fluid velocity squared and inversely proportional the conduct diameter. It is calculated from the Fanning equation (Colebrook and White (1937); Stanley and Mah (1977)), defined for any fluid model by

$$P_{Loss} = \frac{2f\rho v^2 L}{D}, \tag{1}$$

where L is conduct length, v is fluid velocity, ρ is fluid density, and D is conduct diameter. In general, the friction factor f, called the Fanning friction factor, depends on Reynolds number, Re, and the surface conditions of the drillstring which is defined by the roughness of the pipe ε/D. To make it simple, in the paper, it is assumed that L, D and ρ are constant. Then the pressure loss in the drillstring, annulus and riser are defined respectively as

$$P_{Loss,d} = F_d q_d^{n_e}, \tag{2a}$$
$$P_{Loss,a} = F_a q_a^{n_e}, \tag{2b}$$
$$P_{Loss,r} = F_r q_r^{n_e}, \tag{2c}$$

where q_d, q_a, and q_r represents the average flow rate in the drillstring, annulus and riser respectively.

Remark 1. The exponent n_e depends on the flow regime. For instance, n_e is near or close to 1 where flow is laminar and n_e is near 1.75 where flow is turbulent.

Para.	Description	Unit
V_d	Drill string volume	m^3
β_d	Bulk modulus of fluid in drill string	bar
p_p	Pump pressure	bar
q_b	Flow rate of the bit	m^3/s
q_a	Flow rate of the annulus	m^3/s
q_p	Flow rate of the pump	m^3/s
q_s	Flow rate of the subsea pump	m^3/s
F_a	Friction parameter of annulus	$bar\,s^2/m^6$
F_d	Friction parameter of drill string	$bar\,s^2/m^6$
F_r	Friction parameter of riser	$bar\,s^2/m^6$
ρ_a	Density mud in annulus	$10^5 kg/m^3$
ρ_d	Density mud in drill string	$10^5 kg/m^3$
ρ_l	Density mud above mud level	$10^5 kg/m^3$
g	Acceleration of gravity	m/s^2
h	Vertical depth of the bit	m
h_s	Vertical depth from seabed to sea level	m
ℓ	mud height in the mud level in the riser	m
ℓ_a	Length of annulus	m
ℓ_d	Length of drill string	m
A_a	Cross sectional area of annulus	m^2
A_d	Cross sectional area of drill string	m^2
A_r	Cross sectional area of riser	m^2
p_{bit}	Bottom hole pressure	bar

Table 1. Model parameters.

3.2 Mud level dynamics

In the annulus section, from the bottom of the wellbore to the seabed, the heavy mud is extracted by the subsea pump with the flow rate q_s. The mud height from the level to the seabed is defined by ℓ, which is illustrated in Figure 1. The volume of the heavy mud in the riser is given by

$$V = A_r \ell.$$

The flow rate in the riser can be expressed as

$$q_r = q_a - q_s. \tag{3}$$

Then the heavy mud volume dynamics in the riser can be modelled as, see also in Zhou and Nygaard (2011),

$$\frac{dV}{dt} = q_r = q_a - q_s. \tag{4}$$

Assume that the cross sectional area A_r is constant. Then the mud level dynamics in the riser is given by

$$\dot{\ell} = \frac{d\ell}{dt} = \frac{1}{A_r}(q_a - q_s). \tag{5}$$

In the riser section, above the mud level, the riser is full of light liquid with the density ρ_l; below the mud level, the riser is full

of heavy mud with the density ρ_a. Therefore the pressure at the seabed in the riser can be shown as

$$p_{rb} = \rho_a g\ell + \rho_l g(h_s - \ell) + F_r q_r^{n_e}. \quad (6)$$

3.3 Mud density dynamics

During drilling operation the drilling fluid properties are crucial to make safe and efficient drilling process. Various additives for adjusting the drilling fluid density are injected into the drilling fluid to maintain the required fluid properties. In DGD systems, the light mud liquid can be adjusted to make a good complement to keep the safe drilling operations.
In this section, the density model is introduced. More discussions about the model are given in Nygaard and Cimpan (2013). The model is represented by

$$V_t\dot{\rho}_l = -\rho_l\dot{V}_t + \rho_i q_i + \rho_b q_b + \rho_w q_w - \rho_l q_o, \quad (7)$$

where ρ_l is the density of the tank fluid which is filled into the riser above the heavy mud level, V_t is the volume of the tank, ρ_i is the density of the fluid from the wellbore entering the tank (then $\rho_i = \rho_a$), q_i is the volume flow rate of the fluid from the wellbore entering the tank (then $q_i = q_a$), ρ_b is the density of the densifying liquid, q_b is its volume flow rate, ρ_w is the density of the diluting liquid, q_w is its volume flow rate, and q_o is the volume flow rate of the liquid out of the tank.

3.4 Flow hydraulics

For DGD systems we consider a simplified model developed by Kaasa (2007); Stamnes (2007). The model is based on a mass balance for the drill string, and a momentum balance at the drill bit. The pressure dynamics in drill string can be found:

$$\dot{p}_p = \frac{\beta_d}{V_d}(q_p - q_b). \quad (8a)$$

The volume flow dynamics is derived from the momentum balance and is governed by

$$\dot{q}_b = \frac{1}{M}(p_p - p_{rb} - F_a q_b^{n_e} - F_d q_b^{n_e} + \rho_d g h - \rho_a g(h - h_s)), \quad (9)$$

where the parameter $M = M_a + M_d$ with

$$M_a = \rho_a \int_o^{\ell_a} \frac{1}{A_a(x)} dx,$$
$$M_d = \rho_d \int_o^{\ell_d} \frac{1}{A_d(x)} dx.$$

The pressure of the bottom hole, p_{bit}, depends on the friction pressure and hydrostatic pressure, which is finally given as

$$p_{bit} = p_{rb} + \rho_a g(h - h_s) + F_a q_b^{n_e}. \quad (10)$$

3.5 Summary of models

In summary, the DGD system can be described as

$$\begin{aligned}
\dot{p}_p &= \frac{\beta_d}{V_d}(q_p - q_b),\\
\dot{q}_b &= \frac{1}{M}(p_p - p_{rb} - F_a q_b^{n_e} - F_d q_b^{n_e} + \rho_d g h - \rho_a g(h - h_s)),\\
\dot{\ell} &= \frac{1}{A_r}(q_b - q_s),\\
p_{rb} &= \rho_a g\ell + \rho_l g(h_s - \ell) + F_r(q_b - q_s)^{n_e},\\
p_{bit} &= p_{rb} + \rho_a g(h - h_s) + F_a q_b^{n_e}.
\end{aligned}$$

To simplify it, a general DGD control system can be summarized as

$$\dot{x}(t) = f(x(t), u(t)), \quad (11)$$
$$y(t) = g(x(t)), \quad (12)$$

where the state $x(t)$, input $u(t)$, output $y(t)$ are given by

$$x(t) = \begin{bmatrix} p_p(t) \\ q_b(t) \\ \ell(t) \end{bmatrix}, \ u(t) = q_s(t), \ y(t) = p_{bit}(t). \quad (13)$$

4. DRILLING PARAMETERS ANALYSIS

In this section, we focus on the sensitivity analysis for improvement of the design performance. Hence in this section we only discuss the static model. To further simply, it is assumed that

(A1) $q_d = q_a = q_p = q_b$.

From equations (6) and (10) and Assumption (A1), we have

$$p_{bit} = \rho_a g(h - \varsigma) + \rho_l g\varsigma + F_a q_p^{n_e} + F_r(q_p - q_s)^{n_e}, \quad (14)$$

where $\varsigma = h_s - \ell$. It is easy to know that the BHP depends on parameters $\rho_{a(l)}$, ℓ, q_p, $F_{a(r)}$ and q_s. Therefore, we focus on the analysis of the effect of parameters (light liquid density, ρ_l, mud level ℓ, flow rate q_p, and the size of the riser A_r) on the bottom hole pressure p_{bit}, especially under the connection operations.

4.1 Light liquid weight ρ_l and mud level in riser ℓ

During connection, the increase or decrease of the BHP is determined by the increase or decrease of the level. When the level ℓ is given, the available riser length for increase (decrease) is illustrated in Figure 2 (similar figure is shown in Sigurjonsson (2011)). It is easy to know that the maximal length rising is ς. Suppose the setpoint of the BHP is given as $\bar{p}_{bit}$. Given q_p, q_s, ρ_a, and ℓ, from (14), the light liquid weight could be selected according to (15) in order to make the BHP, p_{bit}, close to the setpoint $\bar{p}_{bit}$:

$$\bar{\rho}_l = \frac{\bar{p}_{bit} - \rho_a g(h - \varsigma) - F_a q_p^{n_e} - F_r(q_p - q_s)^{n_e}}{g\varsigma}. \quad (15)$$

When the circulation is stopped, pressure loss in the annulus and riser becomes zero. Then the BHP is only determined by the hydrostatic pressure in the annulus and riser. In order to maintain the stable BHP, the mud level in the riser has to raise to compensate the drop of the BHP. The maximum increase of hydrostatic pressure can be represented as

$$(\rho_a - \rho_l)g\varsigma. \quad (16)$$

To keep the stable BHP, DGD systems must have the sufficient capacity to compensate the pressure loss by increasing hydrostatic pressure. Then one sufficient condition can be

$$(\rho_a - \rho_l)g\varsigma \geq F_a q_p^{n_e} + F_r(q_p - q_s)^{n_e}. \quad (17)$$

Therefore, the choice of light liquid weight could meet the following condition:

$$\rho_l \leq \rho_a - (F_a q_p^{n_e} + F_r(q_p - q_s)^{n_e})/g\varsigma. \quad (18)$$

From the above discussions, the selection of light liquid weight can be summarized as

- ρ_l would be close to the setpoint $\bar{\rho}_l$ given in (15);
- ρ_l has some upper bound from (18).

In section 3.3, the density dynamics is given. Based on the density model, the light liquid density can be easily manipulated with respect to given drilling parameters, for instance, flow rate and mud level.

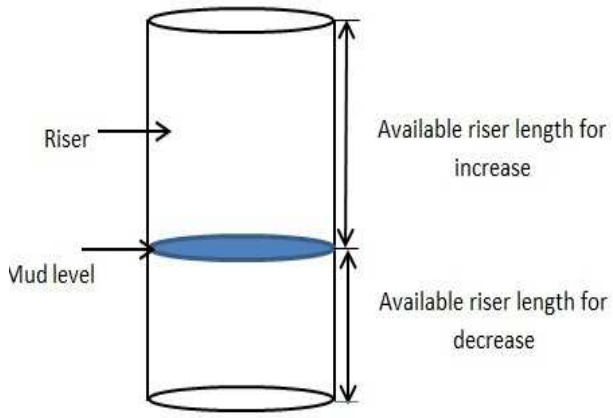

Fig. 2. Available length in riser with respect to mud level.

4.2 Pump rate q_p

During connection, to compensate the drop of the BHP, the mud level in the riser should raise. The change of the mud volume in the riser can be calculated by

$$\Delta V = \int_{t_0}^{t_1} (q_p(t) - q_s(t))dt, \tag{19}$$

where t_0 is the time when the main pump starts ramping down and t_1 is the time when the main pump is fully shut down. The increase length is defined by

$$\Delta \ell = \ell_n - \ell_o = \frac{\Delta V}{A_r}, \tag{20}$$

where ℓ_o is the old stable mud level and ℓ_n is the new stable mud level. Then the increase of hydrostatic pressure is

$$(\rho_a - \rho_l) g \Delta \ell. \tag{21}$$

It is easy to understand that the maximum increase of the mud level happens when $q_s(t) = 0,\ t_0 \le t \le t_1$. Similar as (17), one sufficient condition to keep the steady-state of the BHP unchanged during connections is

$$(\rho_a - \rho_l) g \Delta \ell \ge F_a (q_p(t_0))^{n_e} + F_r (q_p(t_0) - q_s(t_0))^{n_e}, \tag{22}$$

From (21), we obtain

$$\Delta V \ge \frac{A_r}{(\rho_a - \rho_l) g} (F_a (q_p(t_0))^{n_e} + F_r (q_p(t_0) - q_s(t_0))^{n_e}). \tag{23}$$

From (19), we further get that the condition becomes

$$\int_{t_0}^{t_1} q_p(t)dt \ge \frac{A_r}{(\rho_a - \rho_l) g} (F_a (q_p(t_0))^{n_e} + F_r (q_p(t_0) - q_s(t_0))^{n_e}) + \int_{t_0}^{t_1} q_s(t)dt. \tag{24}$$

From (24), we know that a suitable choice of shut down speed $q_p(t)\ t_0 \le t \le t_1$ depends on many factors, $A_r, \rho_a, \rho_l, F_{a(r)}$ and the flow rate $q_p(t_0), q_s(t)$. In the simulation example (see Section 6.2), one specified shut down flow rate satisfying (24) is derived for the illustration.

5. AUTOMATED DGD SYSTEMS

5.1 Model predictive control formulation

Model predictive control is a feedback scheme in which an optimal control problem is solved at each time step and only the first step of the control sequence is applied. The idea of MPC can be summarized as follows: at each control interval, a process model is utilized to predict the future response of a plant, and a constrained optimization problem is then solved to yield a sequence of future manipulated variable control adjustments in order to optimize future plant behavior. The $N+1$ outputs, N inputs and the reference trajectory (set-point trajectory) at time t are denoted as

$$Y(t) = \begin{bmatrix} y(t) \\ \vdots \\ y(t+N) \end{bmatrix},\ U(t) = \begin{bmatrix} u(t) \\ \vdots \\ u(t+N-1) \end{bmatrix},$$
$$Y_{sp}(t) = \begin{bmatrix} y_{sp}(t) \\ \vdots \\ y_{sp}(t+N) \end{bmatrix}. \tag{25}$$

In the MPC formulation, the following cost (26) is minimized to determine the optimal control sequence $U(t)$ in the prediction horizon length N. The MPC formulation can be written as

$$\min_{U(t)} J(t) = (Y(t) - Y_{sp}(t))^T Q (Y(t) - Y_{sp}(t)) + U(t)^T M U(t) \tag{26}$$

subject to

$$x(k+1) = f(x(k), u(k)),\ \ k = t, \ldots, t+N-1, \tag{27}$$
$$y(k) = g(x(k)),\ \ k = t, \ldots, t+N, \tag{28}$$
$$x(k) \in \mathbb{X},\ \ k = t, \ldots, t+N, \tag{29}$$
$$y(k) \in \mathbb{Y},\ \ k = t, \ldots, t+N, \tag{30}$$
$$u(k) \in \mathbb{U},\ \ k = t, \ldots, t+N-1, \tag{31}$$

where Q and M are the tracking and control input weighting matrices in the horizon N; $\mathbb{X}$, $\mathbb{Y}$ and $\mathbb{U}$ are the state, output and input constrained sets respectively. Once the control sequence has been determined, the first one $u(t)$ is applied and the calculation is repeated at the next step.

5.2 MPC implementation

In the section the MPC strategy is implemented to regulate the BHP close to the set point of the BHP. The flow model is summarized in (11)-(13). At time t, the MPC formulation can be written as

$$\min_{U(t)} J(t) = \sum_{k=t}^{t+N} \alpha (y(k) - y_{sp})^2 + \sum_{k=t}^{t+N-1} \gamma q_s^2(k) \tag{32}$$

subject to

$$x(k+1) = f(x(k), u(k)),\ \ k = t, \ldots, t+N-1, \tag{33}$$
$$y(k) = p_{bit}(k),\ \ k = t, \ldots, t+N, \tag{34}$$
$$p_p(k) \ge 0, q_b(k) \ge 0, 0 \le \ell(k) \le h_s,\ \ k = t, \ldots, t+N, \tag{35}$$
$$p_{pore} \le y(k) \le p_{frac},\ \ k = t, \ldots, t+N, \tag{36}$$
$$q_s(k) \ge 0,\ \ k = t, \ldots, t+N-1, \tag{37}$$

where $\alpha > 0, \gamma > 0$ are weighting variables, p_{pore} is the pore pressure and p_{frac} is the fracture pressure.

Remark 2. If drilling parameters shown in Table 1 have high uncertainty, it will result in the increase of the uncertainty of the model (11)-(13) used in the MPC formulation. Then the

horizon window would be recommended to be short to reduce the uncertain information involved in the model.

6. SIMULATION RESULTS

Parameter	Value	Unit
V_d	17	m^3
A_r	0.01	m^2
ρ_a	1580	kg/m^3
ρ_d	1580	kg/m^3
g	9.81	m/s^2
h	2000	m
h_s	1200	m
M	4800	$10^{-5} \times kg/m^4$
F_d	$5*10^9$	–
F_a	$2*10^9$	–
F_r	$2*10^9$	–
β_d	$2*10^4$	–
n_e	2	–
p_{pore}	250	bar
p_{frac}	300	bar
$\bar{p}_{bit}$	280	bar

Table 2. Parameter values for simulation

In this section, the MPC algorithm is applied to the DGD system. The data is sampled at 1Hz. The parameter values for simulation are shown in Table 2.

6.1 Choice of light liquid weight

During circulation, it is assumed that the flow rate of subsea pump equals to the flow rate of main pump. The light liquid density is chosen based on Section 4.1. Table 3 shows the selected values of ρ_l with respect to different ℓ, different flow rate, depth from seabed to sea level and heavy mud density. From Figure 2, we know that it is expected that the mud level

$\rho_l(kg/m^3)$	ℓ(m)	$q_p(l/min)$	$\rho_d(kg/m^3)$	h_s(m)
693	600	2000	1580	1200
1048	200	2000	1580	1200
976	600	1000	1580	1200
1218	200	1000	1580	1200
1047	600	500	1580	1200
1260	200	500	1580	1200
1023	600	2000	1400	1200
250	600	2000	1580	1000

Table 3. Parameter values

is kept in the middle of the riser such that there is enough space for level increasing (decreasing). Under the same situation (q_p, ρ_d, h_s), the larger ℓ, the lighter liquid density is required. Furthermore, the lower the flow rate, the heavier liquid density is required. Then by manipulating light liquid weight following (15) and (18), it provides a good complementary option to manage the wellbore pressure.

6.2 Pump rate reference

During connection suppose the pump ramping rate follows the change

$$q_p(t) = \begin{cases} q_p(t_0) - \bar{q} \times (t - t_0), & t_0 \le t \le t_1 \\ 0, & t_1 \le t \le t_2 \\ \bar{q} \times (t - t_2), & t_2 \le t \le t_3 \end{cases} \quad (38)$$

where $\bar{q}$ is constant. Figure 3 shows the trajectory of pump ramping rate.

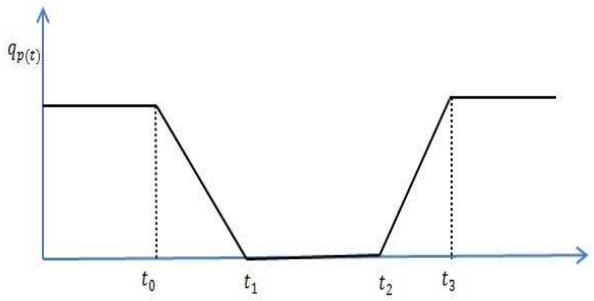

Fig. 3. Pump rate during connection

In the following, we will show how to choose a suitable $\bar{q}$ to make DGD systems keep the stable BHP based on the discussions in section 4.2. Since at time t_1, $q_p(t_1) = 0$. Then we have

$$t_1 = q_p(t_0)/\bar{q} + t_0.$$

Then it is easy to know that

$$\begin{aligned} &\int_{t_0}^{t_1} q_p(t)dt = \int_{t_0}^{t_1} (q_p(t_0) - \bar{q} \times (t - t_0))dt \\ &= \int_0^{t_1 - t_0} (q_p(t_0) - \bar{q} \times t)dt \\ &= q_p(t_0)t|_0^{q_p(t_0)/\bar{q}} - 1/2\bar{q}t^2|_0^{q_p(t_0)/\bar{q}} \\ &= 1/2q_p(t_0)^2/\bar{q}. \end{aligned} \quad (39)$$

If the term in the right side of the inequality (24) is defined as ξ, then we have

$$\begin{aligned} &1/2q_p(t_0)^2/\bar{q} \ge \xi, \\ &\Rightarrow \bar{q} \le 1/2q_p(t_0)^2/\xi. \end{aligned} \quad (40)$$

Suppose $q_p(t_0) = q_s(t_0) = 2000l/min$ and the effect of subsea pump on mud volume in the riser is neglected. Then it is easy to calculate that $\bar{q}$ can be chosen as $400l/min^2$ such that (40) is satisfied.

6.3 BHP management

Let flow rate during circulation be $q_p(t) = q_s(t) = 2000l/min$. The main pump ramping rate satisfies (40) with $\bar{q} = 400l/min^2$. Choose $\rho_l = 1000kg/m^3$ such that the mud level is kept around $280m$ during circulation. By implementing the MPC, the performance of the DGD system is shown in Figure 4-5.

From Figure 5, we know that the mud level is stable at 280m during circulation. With the decrease of flow rate of main pump, the mud level is increasing to compensate the drop of the BHP. When the pump is fully stopped, the mud level is increased to 670m. Then with the pump is ramped up, the riser level is gradually dropping to reduce the hydrostatic pressure in the riser to further keep the stable BHP. Frome Figure 5, the BHP during connection is close to the setpoint 280bar, and its variation is limited within 1bar. Therefore, the simulation shows the good performance of automated DGD systems.

7. CONCLUSION

In this paper, an automated DGD system during connection operations is present. The simulation illustrates that the proposed method is capable to manage the stable BHP during connection

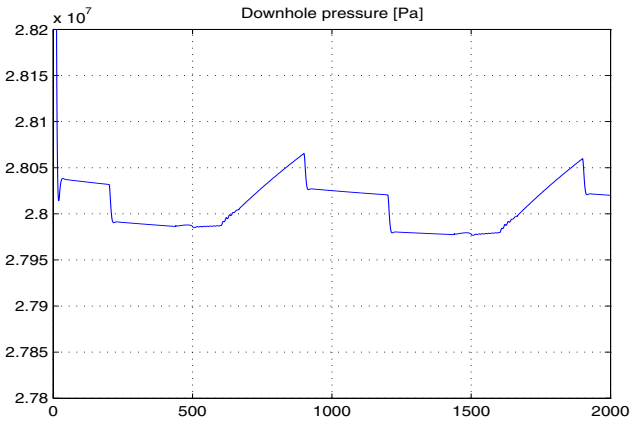

Fig. 4. Dynamic response of the BHP during connections.

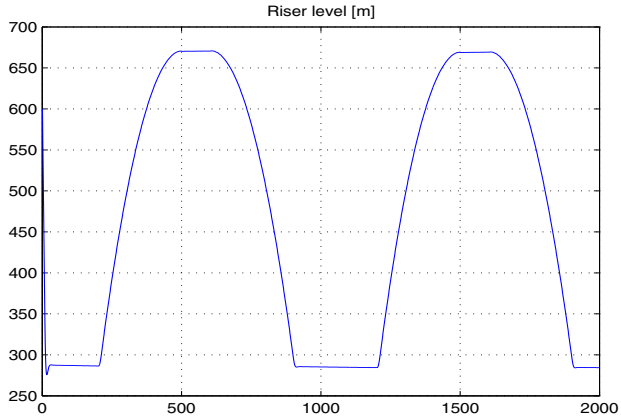

Fig. 5. Dynamic response of the mud level during connections.

and the key parameters which affect the BHP are analyzed and corresponding values for improvement are suggested. The described method might be extended in future work by considering temperature effect and other drilling scenarios.

ACKNOWLEDGMENT

Authors would like to thank Statoil for financial support through the Akademia program. Furthermore, Authors would like to thank Andre Time and Andreas Hanekamhaug who have worked on such DGD topics and helped with the research under their master thesis projects.

REFERENCES

Ø. Breyholtz, G. Nygaard, and M. Nikolaou. Advanced automatic control of dual gradient drilling. In *SPE Annual Technical Conference and Exhibition*, 2009.

Ø. Breyholtz, G. Nygaard, and M. Nikolaou. Managed pressure drilling: using model predictive control to improve pressure control for during dual-gradient drilling. In *SPE Drilling and Completion*, 2011.

C. F. Colebrook and C. M. White. Experiments with fluid friction roughened pipes. *Proc. R.Soc.(A), 161*, 1937.

N. Forrest and T. Bailey. Subsea equipment for deep water drilling using dual gradient mud system. In *SPE/IADC Drilling Conference*, 2001.

C Garcia and M. Prett. Model predictive control: theory and practice. 1989.

T. H. Gaup. Simulations of dual gradient drilling. In *Master thesis, Norwegian University of Science and Technology*, 2012.

J. M. Godhavn, A. Pavlov, and G. O. Kaasa. New automatic control solutions for the drilling industry. In *Transaction on control and mechanical systems*, 2013.

A. . Hanekamhaug. Sensitivity analysis on dual gradient drilling. In *Master thesis, University of Stavanger*, 2015.

G. O. Kaasa. *A simple dynamic model of drilling for control*. Technical report, StatoilHydro Research Centre, Porsgrunn, 2007.

D.Q. Mayne and Michalska. Receding horizon control of nonlinear systems. 1990.

G. Nygaard and E. Cimpan. Simulation and evaluation of the drilling fluid mixing and conditioning process. In *Scandinavian Simulation Society*, 2013.

G. Nygaard, E. A. Johannessen, J. E. Gravdal, and F. Iversen. Automatic coordinated control of pump rates and choke valve for compensating pressure fluctuations during surge and swab operations. In *in SPE Managed Pressure Drilling and Underbalanced Operations*, 2007.

J. P. Schumacher, J. D. Dowell, L. R. Ribbeck, and J. C. Eggemeyer. Planning and preparing for the first subsea filed test of a full-scale dual gradient drilling system. *SPE Drilling and Completion*, 2002.

K. O. Sigurjonsson. Dual gradient drilling simulations. In *Master thesis, Norwegian University of Science and Technology*, 2011.

Ø. N. Stamnes. *Observer for bottomhole pressure during drilling*. Master Thesis, NTNU, 2007.

Ø. N. Stamnes, J. Zhou, G. O. Kaasa, and O. M. Aamo. Adaptive observer design for the bottomhole pressure of a managed pressure drilling system. In *In IEEE Conference on Decision and Control*, 2008.

G. M. Stanley and R. S. H. Mah. Estimation of flows and temperatures in process networks. *AIChE Journal 23*, 1977.

A. Time. Dual gradient drilling- simulations during connection operations. In *Master thesis, University of Stavanger*, 2014.

J. Zhou and G. Nygaard. Automatic model-based control scheme for stabilizing pressure during dual-gradient drilling. *Journal of Process Control*, 2011.

J. Zhou, Ø. N. Stamnes, O. M. Aamo, and G. O. Kaasa. Adaptive output feedback control of a managed pressure drilling system. In *In 47th IEEE Conference on Decision and Control*, 2008.